Drug Design, Development and Therapy

Dovepress
open access to scientific and medical research

Open Access Full Text Article

ORIGINAL RESEARCH

RETRACTED ARTICLE: Orcinol glucoside facilitates the shift of MSC fate to osteoblast and prevents adipogenesis via Wnt/β-catenin signaling pathway

This article was published in the following Dove Press journal:
Drug Design, Development and Therapy

Xinying Zhou
Zezheng Liu
Bin Huang
Huibo Yan
Changsheng Yang
Qingchu Li
Dadi Jin

Department of Orthopedics, The Third Affiliated Hospital, Southern Medical University, Guangzhou, People's Republic of China

Background: During osteoporosis, bone mesenchymal stem cells (BMSCs) lineage commitment shifts to adipocytes, causing fat accumulation and bone loss in the skeleton. Seeking drugs that could reverse the adipocyte fate determination of BMSCs is critical for osteoporosis therapy. As a traditional Chinese medicine, Rhizoma Curculiginis (Xianmao) has been used to treat bone diseases and promote bone health, while the effective constituent of it and the underlying mechanisms are unknown.

Objectives: The aim of this study is to unveil the role of orcinol glucoside (OG), one constituent of Rhizoma Curculiginis, in osteoporosis and BMSCs lineage commitment and to explore the underlying mechanisms.

Methods: Micro-CT and three-point bending test were performed to determine the effect of OG on bone structure and strength. qPCR and Western blot were performed to determine the expression of osteogenic and adipogenic differentiation markers in BMSCs. Mineralization in differentiated BMSCs was assessed by Alizarin Red staining, and lipid accumulation in the cells was evaluated by Oil Red O staining. All measurements were performed at least three times.

Results: OG prevented bone loss by stimulating bone formation and attenuating fat formation in bone. In vitro, OG promoted osteoblastic differentiation and inhibited adipogenic differentiation of BMSCs. Inhibition of Wnt/β-catenin by ICG-001 significantly reversed the effect of OG on osteogenic and adipogenic differentiation of BMSCs.

Conclusion: Our study demonstrated the role of OG in alleviating bone loss and fat accumulation in osteoporotic bone, therefore bringing a new therapeutic means to the treatment of osteoporosis.

Keywords: orcinol glucoside, osteoporosis, mesenchymal stem cell, osteoblast, cell differentiation

Introduction

Osteoporosis, characterized by decreased bone density and bone microarchitecture destruction,[1] is becoming one of the most common skeletal diseases as well as a major public health problem worldwide.[2] During osteoporosis, adipogenesis is increased at the expense of bone formation, resulting in bone loss and fat increase in the bone marrow.[3,4] The disorders in bone and fat formation are mainly due to an imbalance between osteogenic and adipogenic differentiation of multipotential mesenchymal stem cells, the common precursors of osteoblasts and adipocytes in bones.[5,6] Therefore, recovering the osteogenic potential of bone mesenchymal stem cells (BMSCs) could alleviate bone loss and indicates a potential therapeutic strategy for osteoporosis.[7] Seeking drugs that could

Correspondence: Dadi Jin; Qingchu Li
Department of Orthopedics, The Third Affiliated Hospital, Southern Medical University, Academy of Orthopedics, 183 Zhongshan Road West, Guangdong, Guangdong Province 510630, People's Republic of China
Tel +86 206 278 4307
Fax +86 206 278 4332
Email nyorthop@163.com; lqc16@263.net

submit your manuscript | www.dovepress.com
DovePress
http://doi.org/10.2147/DDDT.S208458

regulate BMSC fate determination and clarifying the underlying mechanisms is critical for osteoporosis therapy.

The Wnt/β-catenin pathway, also known as the canonical Wnt pathway, is essential for development and homeostasis and is found to be strongly linked with bone formation.[8,9] Wnt protein acts on its cell surface receptor to prevent β-catenin degradation.[10] Then, the up-regulated β-catenin translocates into the nucleus and stimulates the expression of various downstream genes.[11] Canonical Wnt pathway facilitates osteogenic differentiation of BMSCs by activating the expression of Runt-related transcription factor 2 (RUNX2)[12] and suppresses peroxisome proliferator-activated receptor-γ transcription to inhibit adipogenic differentiation of BMSCs.[13] Thus, drug modulation of Wnt/β-catenin signaling pathway is beneficial for bone turnover and osteoporosis treatment.

Traditional Chinese medicine has been used to treat bone diseases and to promote bone healing, among which Rhizoma Curculiginis (Xianmao) is a well-known "bone-tonifying" herb. Rhizoma Curculiginis has been used to treat limpness of the limbs, arthritis of the lumbar and knee joints, and to strengthen tendons and bones.[14] In particular, Rhizoma Curculiginis extract has been reported to increase bone mass and density in mouse and induce new bone formation in a bone defect mouse model.[14] The limitations of previous studies are that they did not identify the effective constituent of Rhizoma Curculiginis and have not explored the mechanisms responsible. Orcinol glucoside (OG) is an active constituent isolated from Rhizoma Curculiginis.[15] OG has been reported to exert antilipolytic[16] and antidepressive[17] effects in mouse, it is not known whether it has any role in bones. Here, we show that OG alleviated bone loss in ovariectomized mice by stimulating bone formation and inhibiting fat accumulation in bones. OVX caused a shift of BMSC cell lineage commitment to adipocyte, while OG prevented this shift of BMSCs and led them to osteogenic differentiation. Mechanistically, OG activates β-catenin and promotes its translocation into the nucleus in BMSCs. We further prove that OG controlled BMSCs differentiation via Wnt/β-catenin signaling pathway since the effect of OG on BMSCs differentiation was abrogated by ICG-001, a Wnt/β-catenin agonist.

Materials and methods

Animals

We purchased 8-week female C57BL/6 mice from the Laboratory Animal Research Center of the Southern Medical University. Mice importation, transportation, housing and breeding were conducted according to the recommendations of "The use of non-human primates in research". The mice were randomly divided into sham, OVX and OVX + OG groups. Sham surgery and bilateral surgical ovariectomy (OVX) were performed by dorsal approach under general anesthesia. Mice in the OVX + OG group (n=10) were administered intragastrically with OG (Selleck, 10 mg/kg/day, dissolved by normal saline to a working concentration of 0.5 g/L) for 3 months after OVX. Mice in the other two groups were treated with vehicle after OVX. To prevent suffering, the mice were killed by cervical dislocation. All procedures have been approved by the Animal Care Committee of the Southern Medical University and have met the NIH guidelines for care and use of laboratory animals in this study.

Three-point bending test

The tibia was placed in a holder that fixed the ends of the bone in place while a measured amount of force was applied perpendicular to the midpoint of the anterior side of the tibial diaphysis. Load was applied with a rate of 0.1 mm/s until the fracture occurred. Data were analyzed to determine values of stiffness, ultimate load and Young's modulus using the following formula: Young's modulus = (Stiffτ. Ls3)/48.I, where Stiffτ is the stiffness, Ls is the separation of the supports and I is the second moment of area of the tibias. The stiffness was calculated by measuring the slope of the force–displacement graph and the ultimate load by measuring the maximum force that the bone was able to resist. The second moment of area was calculated using the microCT data and Image J software and the plug-in Bone J.

Micro-CT scanning and analysis

Femurs were wiped off all surrounding soft tissues and fixed by 4% phosphate-buffered paraformaldehyde immediately. Bone structure was analyzed by a micro-CT system (Viva CT40; Scanco Medical AG, Bassersdorf, Switzerland).[18] Briefly, scanning was performed at the lower growth plate in the femora and extended proximally for 300 slices. Morphometric analysis was started with the first slice in which the femoral condyles were fully merged and extended for 100 slices proximally. The trabecular bone was segmented from the cortical shell manually on key slices using a contouring tool, and the contours were morphed automatically to segment the trabecular bone on all slices. Trabecular parameters included trabecular bone

mineral density (BMD, mg HA/ccm), bone volume fraction (BV/TV, percent), number (Tb.N, number per millimeter), thickness (Tb.Th, micrometer) and separation (Tb.Sp, micrometer).

Preparation of decalcified sections, histochemistry and immunohistochemistry (IHC) analyses

Femur tissues were then decalcified in 15% EDTA (pH 7.4) at 4°C for 14 days. The tissues were embedded in paraffin, and 5-μm sagittal-oriented sections were prepared for histological analyses. H&E staining was performed as previously described.[19] Tartrate-resistant acid phosphatase (TRAP) staining was performed using a standard protocol (Sigma-Aldrich). For IHC, we incubated primary antibodies which recognized mouse Runx2 (Cell Signaling, 1:100) and osteocalcin (Abcam, 1:500, ab93876) overnight at 4°C. All sections were observed and photographed on an Olympus BX51 microscope. Immunohistochemical staining was evaluated by positive cell number per bone perimeter. At least six different images at 40× magnification for IHC staining were taken and evaluated by using ImageJ Pro.

BMSCs

We isolated and cultured mouse BMSCs as previously described.[20] The cells were thawed and seeded in α-minimum essential medium (Gibco, Invitrogen, USA), 10% FBS (Gibco, Invitrogen, USA), 2 mM/L L-glutamine (Invitrogen, Carlsbad, CA), 100 U/mL penicillin and 100 mg/mL streptomycin (Invitrogen, Carlsbad, CA). Cells were incubated in a humidified incubator containing 5% CO_2 at 37°C and the medium was changed every 3 days. BMSCs were passaged by 0.25% trypsin until confluence. For osteogenic induction, 10–8 M dexamethasone (Sigma-Aldrich), 50 μg/mL ascorbic acid (Sigma-Aldrich) and 10 mM β-glycerol phosphate (Sigma-Aldrich) were added to confluent cells, while the adipocytic differentiation media contained 10−6 M dexamethasone, 0.5 mM isobutylmethylxanthine, 100 μM indomethacin and 10 mg/L insulin. OG (Selleck) was added as stated in the Results section.

Cell staining

Cells were fixed in 4% paraformaldehyde for 20 mins at room temperature. For ALP staining, osteogenic differentiated BMSCs were washed, incubated with ALP staining buffer (NBT-BCIP, Sigma-Aldrich) at 37°C for 30 mins and washed with PBS to remove excess dye. For Alizarin Red staining, the fixed cells were washed with water and stained in Alizarin Red solution (Merck Millipore) for 30 mins at room temperature. Oil Red O staining was performed to detect lipid droplets as described previously.[21]

Real-time reverse transcription-polymerase chain reaction

Total RNA was isolated from cell pellets with TRIzol Reagent (Life Technologies, #15596-018) and reverse transcribed (2.5 mg per sample in a 50 mL reaction volume) using PrimeScript Reverse Transcriptase according to the manufacturer's protocol (Takara, #2680B). A volume of 2 mL of cDNA (corresponding to 100 ng of total RNA) was used for real-time PCR using SYBR Premix Ex Taq (Takara, #RR420A). The primer sequences used are shown in Table 1. PCR amplification program was run at 94°C for 3 mins, at 94°C for 15 and at 60°C for 30 s, 40 cycles. Relative gene expression was determined using the -ΔΔct method versus the housekeeping gene GAPDH.

Western blot assay

Cells were lysed in 2% sodium dodecyl sulfate with 2 M urea, 10% glycerol, 10 mM Tris-HCl (pH 6.8), 10 mM dithiothreitol and 1 mM phenylmethylsulfonyl fluoride. The lysates were centrifuged and the supernatants were separated by SDS-PAGE and blotted onto a nitrocellulose membrane (Bio-Rad Laboratories). The membrane was then incubated with specific antibodies to Runx2 (Cell Signaling

Table 1 PCR primers

Gene	Strand	Sequence (5′′ to 3′′)
Runx2	Forward	AGGGACTATGGCGTCAAACA
	Reverse	GGCTCACGTCGCTCATCTT
Ocn	Forward	CAGACACCATGAGGACCATC
	Reverse	GGACTGA GGCTCTGTGAGGT
Osx	Forward	CGCTTTGTGCCTTTGAAAT
	Reverse	CCGTCAACGACGTTATGC
PPAR-γ	Forward	GGAAGACCACTCGCATTCCTT
	Reverse	GTAATCAGCAACCATTGGGTCA
C/EBPα	Forward	CAAGAACAGCAACGAGTACCG
	Reverse	GTCACTGGTCAACTCCAGCAC
Adiponectin	Forward	TGTTCCTCTTAATCCTGCCCA
	Reverse	CCAACCTGCACAAGTTCCCTT
GAPDH	Forward	GCA CAG TCA AGG CCG AGA AT
	Reverse	GCC TTC TCC ATG GTG GTG AA

Technology, #12556S, 1:1,000), Osteocalcin (Abcam, #ab76690, 1:1,000), peroxisome proliferator-activated receptor gamma (PPARγ, Cell Signaling Technology, #2443, 1:1,000), C/EBPα (Cell Signaling Technology, #8178, 1:1,000) and adiponectin (Abcam, #ab22554, 1:2,000). The membrane was then visualized by enhanced chemiluminescence (ECL Kit, Amersham Biosciences).

Statistics

All results are presented as the mean ± SD Curve analysis was determined using Prism (GraphPad). The data in each group were analyzed using unpaired, two-tailed Student's *t*-test. The level of significance was set at $P<0.05$.

Results

OG prevents bone loss in ovariectomized mice

Firstly, we constructed osteoporosis mouse model by bilateral ovariectomy (OVX) (Figure S1A), which is a widely used animal model resembles menopausal osteoporosis in human.[22] Two months after surgery, OVX mice exhibited significant body weight gain (Figure S1B), suggesting a loss of ovary function in the mice and successful model establishment. Accordingly, images from microCT test of femoral metaphysis showed a signi[illegible]ecular bone loss in the femurs of OVX mice (Figure 1A). [illegible]nalysis of representative samples indicated t[illegible] OVX si[illegible]nificantly

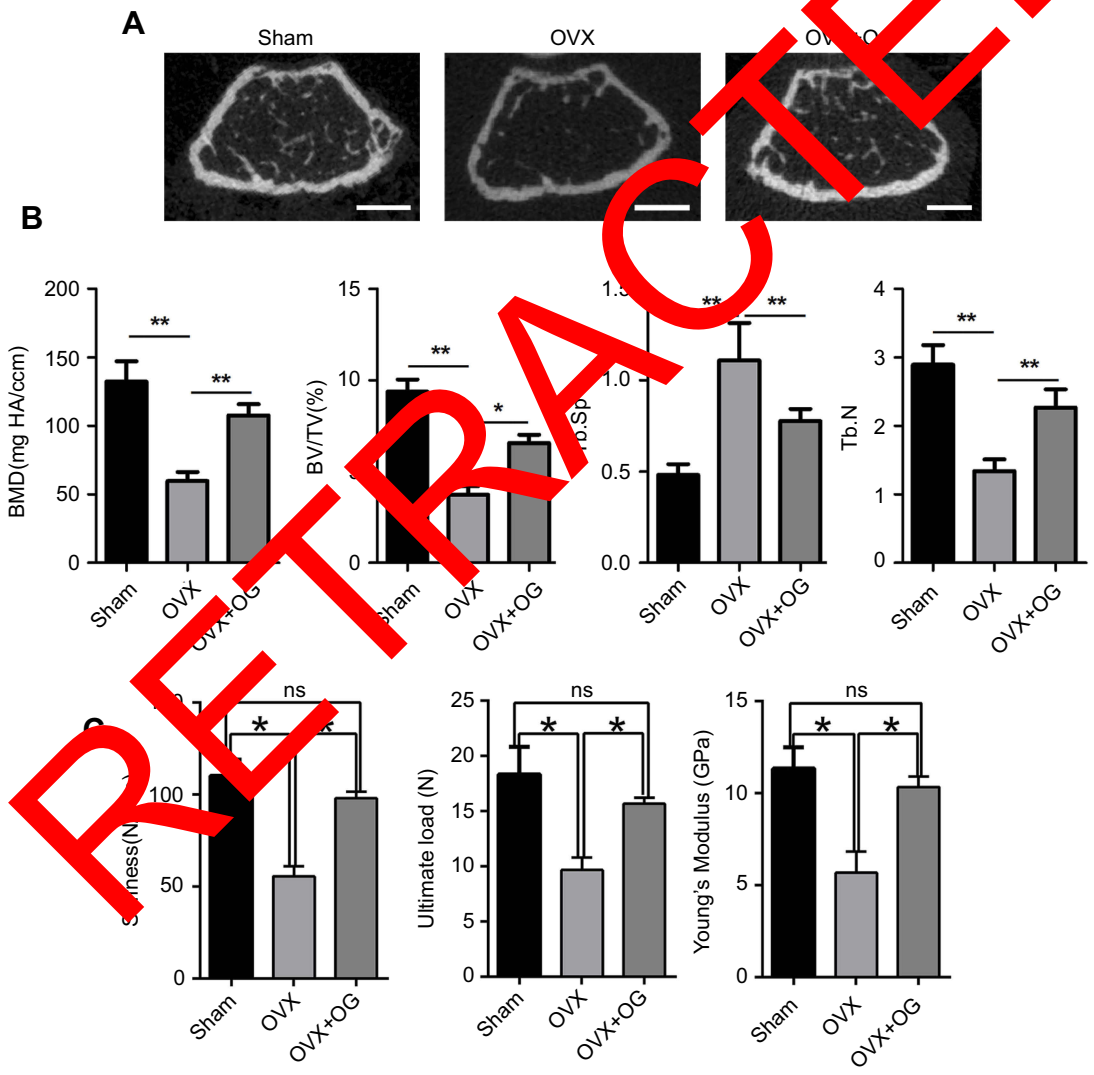

Figure 1 Orcinol glucoside (OG) prevents bone loss in OVX mice. (**A**) Representative images of micro-CT analysis of the structure of metaphyseal trabecular bone in the distal femur showed bone loss in OVX mice and regain of bone mass in OVX mice fed with OG (OVX+OG). (**B**) The structure parameters were calculated. Scale bar: 1 mm (n=5 mice for each group). (**C**) Three-point bending test showed that stiffness, ultimate load and Young's modulus were all reduced in OVX mice tibias, while OG administration reversed the reduction of these parameters. *p<0.05, **p<0.01. Plots show mean ± SD.

Abbreviation: ns, not significant.

decreased the trabecular BMD, BV/TV, Tb.N and Tb.Th levels of mice bone (Figure 1B). We also performed a three-point bending test to determine the effects of OVX on mouse tibia bone strength. It revealed reduced structure stiffness, ultimate load and Young's modulus measures in OVX mice (Figure 1C). To test the anti-osteoporosis role of OG, we fed OVX mice with OG after surgery. Oral administration of OG resulted in regain of trabecular bone mass (Figure 1A), preservation of the trabecular bone architecture (Figure 1B) and promotion of bone strength (Figure 1C) significantly but no change in the body weight (Figure S1B) was observed in OVX mice.

OG stimulated osteogenesis and inhibited adipogenesis in mice bone

We then sought to determine how OG influenced bone mass in OVX mice. As osteoblasts are the main bone-forming cells, we firstly detected the variation of osteoblast number in the bones. Immunostaining of markers of osteoblasts, Runx2 (Figure 2A and C) and osteocalcin (Figure 2B and D) showed that OG increased osteoblast number in OVX bone. Bone loss in OVX mice is also related to elevated bone resorption, and we thus determined whether osteoclast number was affected by OG. TRAP staining showed that osteoclast number remained unchanged in OG-OVX mouse bone (Figure 2E and G). Excessive adipogenesis in bone marrow also contributes to the pathogenesis of osteoporosis, and we then evaluated the fat mass in mouse bone. As shown in Figure 2F and H, OG reduced bone marrow fat in OVX mice.

OG promoted osteoblastic differentiation of BMSC in vitro

To determine whether the shift of BMSC cell lineage commitment to adipocyte contributes to the bone loss and fat accumulation in osteoporotic bone marrow, we isolated BMSCs from mouse femurs and induced them for osteogenic or adipogenic differentiation. OVX BMSCs

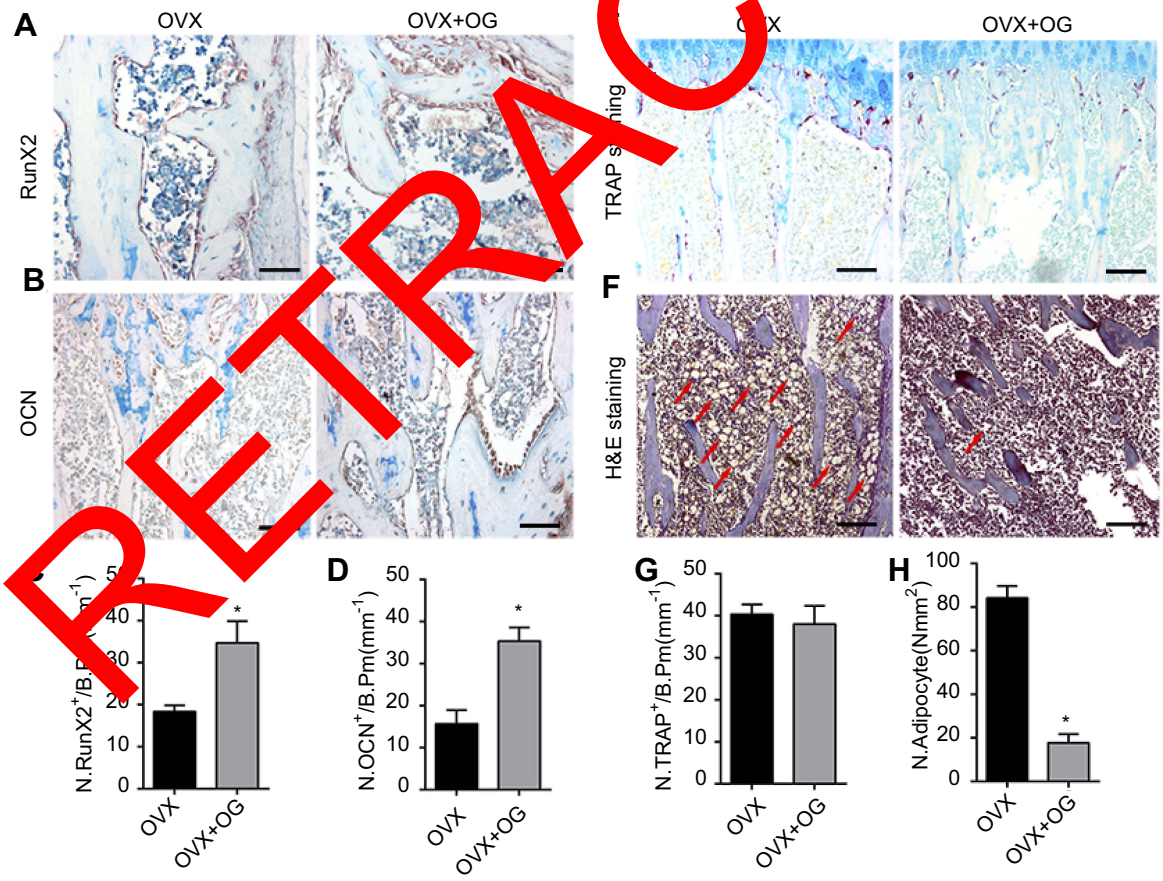

Figure 2 Orcinol glucoside (OG) promoted osteoblast formation and inhibited lipid formation in mice bone. Representative images of immunostaining of (**A**) Runx2 and (**B**) osteocalcin (OCN) and positive cells on the bone surface were measured as cells per millimeter of perimeter in sections (/B.Pm) (**C, D**). TRAP (**E**) and H&E (**F**) staining of mice distal femur. The number of osteoclasts (N.TRAP+) on the bone surface (/B.Pm) (**G**) and adipocytes in the bone marrow (**H**) was measured. Scale bars represent 100 μm in (**A**), (**B**), (**E**) and 200 μm in (**F**). *p<0.05. All data are mean ± SD.

formed less mineralization nodules as revealed by Alizarin Red staining (Figure 3A), whereas they generated more lipid droplets (Figure 3B), compared with SHAM BMSCs. Thus, OVX BMSCs impaired osteoblastic differentiation but facilitated adipocyte differentiation capacity. We then analyzed whether OG increased osteoblast number in mouse bone by promoting osteoblast formation from BMSCs. Ki-67 staining revealed that OG exerted no effects on BMSC proliferation (Figure S2). However, osteoblastic differentiation of the cells was markedly enhanced by OG, as OG-treated BMSCs exhibited an increased amount of Runx2 and Osteocalcin mRNA (Figure 3C) and protein (Figure 3D) expression. The influence of OG on the development of the osteoblast phenotype from MSCs was evaluated by monitoring the formation. When OG was added to the osteogenic medium, the phosphatase alkaline staining showed an increase in comparison with cells not treated with OG (Figure 3E). Moreover, Alizarin Red staining proved facilitated mineralization of BMSCs by OG (Figure 3F). These results OG favors osteoblastic differentiation of BMSCs.

OG attenuated adipocytic differentiation of BMSC in vitro

We also determined the role of OG in the differentiation of BMSCs into adipocytes. We studied the expression of three marker genes for adipogenesis—the transcription factor PPARγ, C/EBPα and adiponectin during adipogenic differentiation of BMSCs. qPCR analysis showed that mRNA expressions of these three markers in BMSCs were all inhibited by OG treatment (Figure 4A). Moreover, protein levels of the three markers were also suppressed by OG (Figure 4B). In addition, the influence of OG on the adipocyte phenotype was evaluated. The formation of lipid droplets, a characteristic of the adipocyte formation process, was monitored using the Oil Red O staining. As shown in Figure 4C, BMSCs treated with OG presented less development of fat in the cells. These results suggested the inhibitory role of OG on adipogenic differentiation of BMSCs.

OG activated Wnt/β-catenin signaling in BMSCs

We then explored the mechanisms responsible for the regulation of BMSCs osteoblastic/adipocytic differentiation by OG. Wnt/β-catenin signaling has been reported to facilitate osteogenic differentiation and to attenuate adipogenic differentiation of BMSCs. Inhibition of Wnt/β-catenin signaling is closely related to osteoporosis. We thus investigated whether Wnt/β-catenin signaling in BMSCs is involved in the development of osteoporosis. Western blot analysis showed a decreased level of active β-catenin (α-ABC) and unchanged total β-catenin levels in OVX BMSCs, while OG treatment increased the α-ABC level to normal (Figure 5A). The function of many transcription factors is associated with changes in their intracellular localization between the cytoplasm and the nucleus. We then found that OG treatment led to α-ABC accumulation in the nucleus of BMSCs (Figure 5B), which promoted the transcriptional activity of α-ABC. These

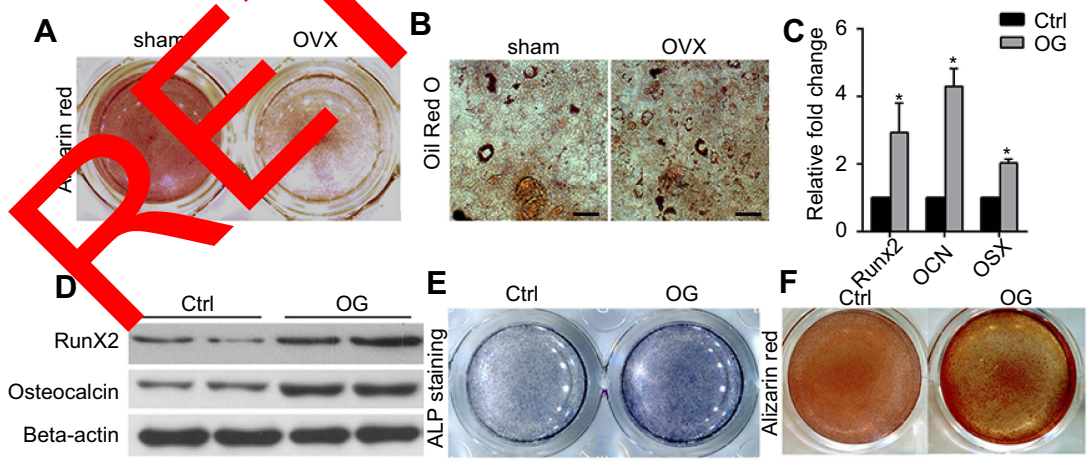

Figure 3 Orcinol glucoside (OG) promoted osteoblastic differentiation of bone mesenchymal stem cell (BMSC) in vitro. (**A**) Alizarin Red staining of osteogenic differentiated BMSC obtained from SHAM and OVX mice bone marrow. (**B**) Oil Red O staining of adipogenic differentiated BMSC collected from mice bone marrow showed decreased lipid formation in OVX BMSCs as compared with sham BMSCs. (**C**) qPCR analysis showed increased Runx2, OCN and osterix (OSX) mRNA expression in BMSCs treated with OG versus their control (Ctrl) treated with PBS. *p<0.05. Data are mean ± SD. (**D**) Western blot analysis showed elevated protein level of Runx2 and osteocalcin in BMSCs treated with OG versus their control (Ctrl). (**E**) ALP staining showed enhanced OB differentiation of BMSCs by OG. (**F**) Alizarin Red staining proved facilitated mineralization of BMSCs by OG.

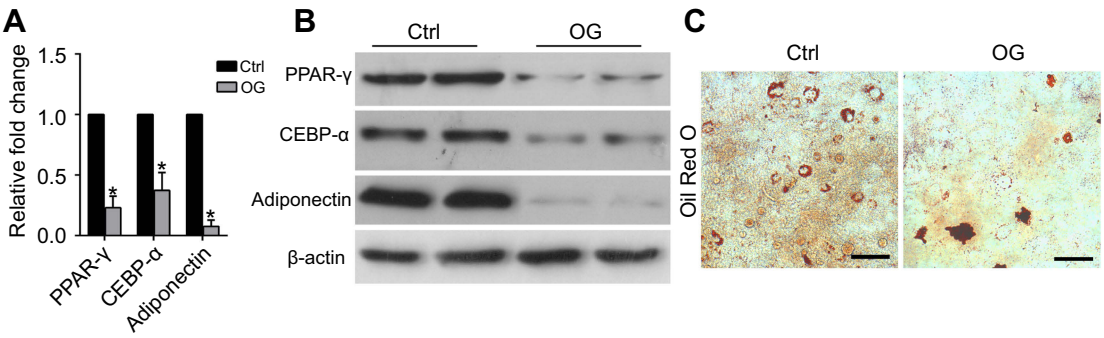

Figure 4 Orcinol glucoside (OG) attenuated adipocytic differentiation of bone mesenchymal stem cell (BMSC) in vitro. (**A**) qPCR analysis showed increased mRNA level of PPAR-γ, CEBP-α and adiponectin in BMSCs treated with OG. (**B**) Western blot analysis of PPAR-γ, CEBP-α and adiponectin showed inhibited adipocytic differentiation of BMSCs by OG. (**C**) Oil Red O staining proved attenuated lipid formation in BMSCs by OG.

findings suggest that OG activated Wnt/β-catenin signaling in BMSCs.

Wnt/β-catenin mediated the effects of OG on lineage commitment of BMSCs

We next determined whether Wnt/β-catenin mediated the effect of OG on BMSCs differentiation. As mentioned above, OG promoted osteoblastic markers, Runx2 and Osteocalcin, expression in BMSCs. This promotion effect on osteoblastic differentiation was abrogated by ICG-001 (a Wnt/β-catenin agonist[24]) (Figure 6A). Moreover, ALP staining also showed that the facilitated differentiation of BMSCs by OG was reversed by ICG-001 (Figure 6B). These results suggested that OG promoted osteoblastic differentiation of BMSCs via Wnt/β-catenin signaling pathway. Wnt/β-catenin signaling pathway also mediated the inhibitory role of OG on adipogenic differentiation of BMSCs, since the suppressed adipogenic differentiation (Figure 6C) and lipid droplet formation (Figure 6D) of BMSCs by OG were significantly abrogated by Wnt signaling inhibition. Taken together, OG recovers bone formation/fat formation disorder of BMSCs during OVX by stimulating Wnt/β-catenin signaling pathway. The Results section describes the most important findings of the study, analysis of experiment. The most important results are indicated, and relevant trends and patterns are described.

Discussion

According to Chinese medicine theories, Rhizoma Curculiginis is "Yang-tonifying" herb that acts on Shen (kidney). Shen is related to bones in traditional Chinese medicine, and thus, Rhizoma Curculiginis affects bone metabolism expectedly. However, these effects had not been demonstrated by modern scientific methods and it is unknown which active constituent of it exerts the effects. In the present study, we investigated the skeletal effects of OG (Figure S3) on osteoporotic mice and explored the possible mechanisms.

In order to evaluate the effect of OG on osteoporosis, we utilized OVX mouse model. OVX mouse imitates postmenopausal osteoporosis in human, which is caused

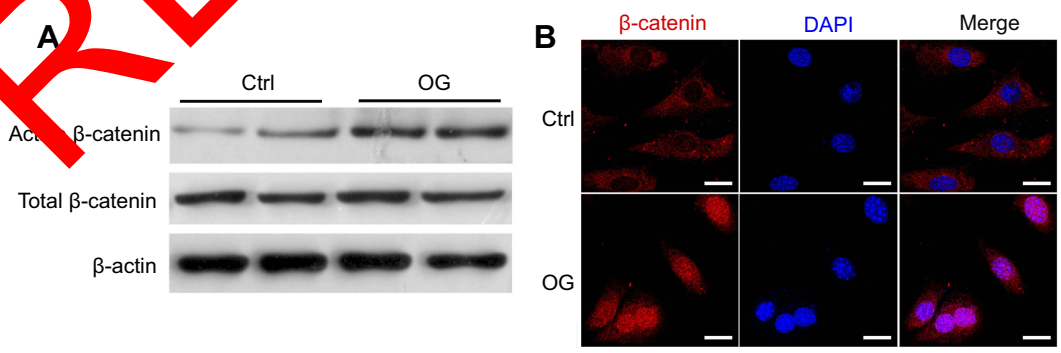

Figure 5 Orcinol glucoside (OG) activated Wnt/β-catenin signaling in bone mesenchymal stem cells (BMSCs). (**A**) Western blot analysis of active β-catenin and total β-catenin levels in BMSCs treated with PBS (Ctrl) or OG. (**B**) Immunofluorescence staining of β-catenin showed that OG promoted the nuclear translocalization of β-catenin in BMSCs.

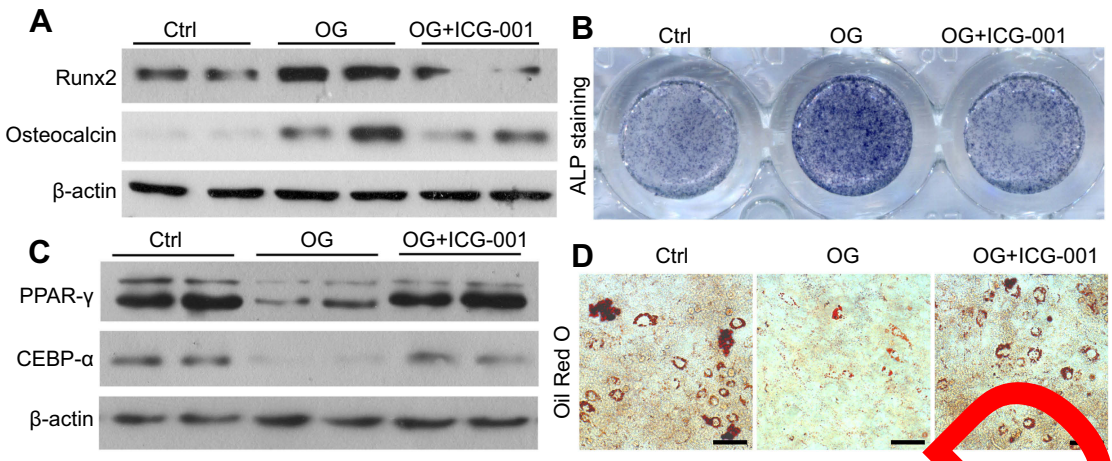

Figure 6 Wnt/β-catenin mediated the effects of orcinol glucoside (OG) on lineage commitment of bone mesenchymal stem cells (BMSCs). (**A**) Cell lysis of osteogenic differentiated BMSCs treated with OG or OG and ICG-001 (Wnt/β-catenin agonist) was subjected to Western blot analysis of Runx2 and osteocalcin (OCN). (**B**) ALP staining of BMSCs induced for osteogenic differentiation on the 7th day. (**C**) Cell lysis of adipogenic differentiated BMSCs treated with OG or OG and ICG-001 was subjected to Western blot analysis of PPAR-γ and CEBP-α. (D) Oil Red O staining adipogenic differentiated BMSCs showed the attenuated lipid formation in BMSCs by OG was reversed by ICG-001.

by estrogen deficiency. Estrogen depletion enhances bone resorption and subsequently stimulates bone formation. The levels of increase of bone resorption exceed those of bone formation in the estrogen-depleted condition, thus causing a net reduction of bone mass.[25] Current therapies for postmenopausal osteoporosis are limited to anti-resorptive agents. Although such agents would generally be considered beneficial, biomechanical bone competence may be compromised if bone resorption is excessively inhibited.[26] In this study, OG prevented bone loss in OVX mice by stimulating bone formation by BMSCs without affecting bone resorption. Thus, results from three-point bending test revealed the maintenance of the biomechanical property of OVX mice bone. As a bone formation stimulator, OG might be a targeted drug for bone diseases due to reduced osteoblast activity, such as senile osteoporosis.

Besides elevated bone resorption, OVX mice also exhibited fat accumulation in bone marrow in this study, which is in agreement with previous studies.[27] Further investigation revealed that osteogenic differentiation defect and facilitated adipogenic differentiation of endogenous BMSCs contributed to the decreased bone volume and increased fat mass in OVX mice. Moreover, recent advances in the elucidation of the pathophysiology of osteoporosis in the elderly indicate that the loss of balance between osteoblastogenesis and adipogenesis in bone marrow cell differentiation is also a key mechanism of osteoporosis in older adults.[28] As a potential drug being able to recover the osteogenic differentiation capacity of BMSCs, OG might also be effective in treating age-related osteoporosis. Moreover, OG might be also safe for the body, as it did not affect the body weight of mice in the present study.

Wnt signaling is crucial for BMSC differentiation and bone formation. Various factors affected osteoblast differentiation and bone formation via Wnt signaling. Our mechanistic study revealed that OG activates Wnt/β-catenin signaling in BMSCs. Previous studies revealed that OG has antioxidative properties,[29,30] and Almeida et al reported that oxidative stress antagonizes Wnt signaling in osteoblast precursors.[31] These findings provide an explanation for Wnt/β-catenin activation in BMSCs by OG in the present study.

Conclusion

Taken together with this study, we revealed here that OG rescued the dysfunction of BMSCs and attenuated bone loss during osteoporosis via activating Wnt/β-catenin signaling pathway, indicating that OG is a potential candidate for developing a drug for osteoporosis treatment.

Abbreviation list

BMSC, bone mesenchymal stem cell; C/EBP, CCAAT-Enhancer-Binding Proteins; MSC, mesenchymal stem cell; OG, orcinol glucoside; OVX, bilateral surgical ovariectomy; PPARγ, peroxisome proliferator-activated receptor gamma; RUNX2, Runt-related transcription factor 2; TRAP, Tartrate-resistant acid phosphatase.

Acknowledgment

This work was supported by grants 81672120 and 81700783 from National Natural Science Foundation of

China and a breeding program of "National Science Fund for Outstanding Youth" granted by the Third Affiliated Hospital of Southern Medical University (BH).

Disclosure

The authors declare that there are no conflicts of interest in this work.

References

1. Nih Consensus Development Panel on Osteoporosis Prevention D, Therapy. Osteoporosis prevention, diagnosis, and therapy. *JAMA*. 2001;285(6):785–795. doi:10.1001/jama.285.6.785
2. Sözen T, Özışık L, Başaran NÇ. An overview and management of osteoporosis. *Eur J Rheumatol*. 2017;4(1):46–56. doi:10.5152/eurjrheum.2016.048
3. Astudillo P, Rios S, Pastenes L, Pino AM, Rodriguez JP. Increased adipogenesis of osteoporotic human-mesenchymal stem cells (MSCs) characterizes by impaired leptin action. *J Cell Biochem*. 2008;103(4):1054–1065. doi:10.1002/jcb.21516
4. Idris AI, Sophocleous A, Landao-Bassonga E, et al. Cannabinoid receptor type 1 protects against age-related osteoporosis by regulating osteoblast and adipocyte differentiation in marrow stromal cells. *Cell Metab*. 2009;10(2):139–147. doi:10.1016/j.cmet.2009.07.006
5. Bianco P, Robey PG, Simmons PJ. Mesenchymal stem cells: revisiting history, concepts, and assays. *Cell Stem Cell*. 2008;2(4):313–319. doi:10.1016/j.stem.2008.03.002
6. Caplan AI. Adult mesenchymal stem cells for tissue engineering versus regenerative medicine. *J Cell Physiol*. 2007;213(2):3[illegible] doi:10.1002/jcp.21200
7. Bergman RJ, Gazit D, Kahn AJ, Gruber H, McDougall S, Hal[illegible] TJ. Age-related changes in osteogenic stem cells in mi[illegible] *J Bone Miner Res*. 1996;11(5):568–577. doi:10.1002/jbmr.565[illegible]1050[illegible]
8. Krishnan V, Bryant HU, Macdougald OA. [illegible]gulation [illegible] bone mass by Wnt signaling. *J Clin Invest*. [illegible]06;116[illegible]299. doi:10.1172/JCI28551
9. Maupin KA, Droscha CJ, William[illegible]O. A compr[illegible]nsive overview of skeletal phenotypes associate[illegible]vi[illegible]lterations in W[illegible]/beta-catenin signaling in humans and [illegible]mice. *B[illegible] Res*. 2013;1(1):27–71. doi:10.4248/BR20130100[illegible]
10. He X, Semenov M, Ta[illegible]d K, Zeng X. LDL r[illegible]tor-related proteins 5 and 6 in Wnt/[illegible]ta-catenin [illegible]ignaling: arrows point the way. *Development*. 2004;[illegible]31(8):1[illegible]5–1677. doi:10.1242/dev.01117
11. Hurlstone A, Clevers [illegible]cell factors[illegible]urn-ons and turn-offs. *Embo J*. 2002;21[illegible]9):2[illegible]03–231[illegible]doi:10.[illegible]93/emboj/21.10.2303
12. Gaur T[illegible]engner [illegible], Hovhan[illegible]n H, et al. Canonical WNT signaling [illegible]motes [illegible]eogenesis by directly stimulating Runx2 gene expres[illegible]. *J[illegible]iol Chem*. [illegible]005;280(39):33132–33140. doi:10.1074/jbc.M500[illegible]200
13. Bennett CN, [illegible]ngo KA, Wright WS, et al. Regulation of osteoblastogenesis and [illegible]e mass by Wnt10b. *Proc Natl Acad Sci U S A*. 2005;102(9):3324–3329. doi:10.1073/pnas.0408742102
14. Wong RW, Rabie B, Bendeus M, Hagg U. The effects of Rhizoma Curculiginis and Rhizoma Drynariae extracts on bones. *Chin Med*. 2007;2:13. doi:10.1186/1749-8546-2-13
15. He Y, Dong X, Jia X, et al. Qualitative and quantitative analysis on chemical constituents from Curculigo orchioides using ultra high performance liquid chromatography coupled with electrospray ionization quadrupole time-of-flight tandem mass spectrometry. *J Pharm Biomed Anal*. 2015;102:236–245. doi:10.1016/j.jpba.2014.09.024
16. Wang X, Li G, Li P, Huang L, Huang J, Zhai H. Anxiolytic effects of orcinol glucoside and orcinol monohydrate in mice. *Pharm Biol*. 2015;53(6):876–881. doi:10.3109/13880209.2014.946060
17. Ge JF, Gao WC, Cheng WM, et al. Orcinol glucoside produces antidepressant effects by blocking the behavioural and neuronal deficits caused by chronic stress. *Eur Neuropsychopharmacol*. 2014;24(1):172–180. doi:10.1016/j.euroneuro.2013.05.007
18. Hildebrand T, Laib A, Muller R, Dequeker J, Ruegsegger P. Direct three-dimensional morphometric analysis of human cancellous bone: microstructural data from spine, femur, iliac crest, and calcaneus. *J Bone Miner Res*. 1999;14(7):1167–1174. doi:10.1359/jbmr.1999.14.7.1167
19. Ye L, Mishina Y, Chen D, et al. Dmp1-deficient mice display severe defects in cartilage formation responsible for a chondrodysplasia-like phenotype. *J Biol Chem*. 2005;280(7)[illegible]6203. doi:10.1074/jbc.M412911200
20. Liu W, Qi M, Konermann A, Zh[illegible]g L, Jin F, Jin[illegible]The p53/miR-17/Smurf1 pathway mediates ske[illegible]l deformities [illegible] an age-related model via inhibiting th[illegible]function[illegible]f mesench[illegible]mal stem cells. *Aging*. 2015;7(3):205–2[illegible]. doi:10.1863[illegible]ging[illegible]0728
21. Song L, Liu M, Ono[illegible], Bringhu[illegible]FR, Ki[illegible]berg HM, Guo J. Loss of wnt/beta-catenin[illegible]malin[illegible]auses cell fate shift of preosteoblasts from osteobla[illegible]to adi[illegible]es. *J Bone [illegible]ner Res*. 2012;27(11):2344–2358. doi:[illegible]002/jbmr.[illegible]
22. Bouxsei[illegible]M[illegible]Myers KS, [illegible]z KL, Donahue LR, Rosen CJ, Beam[illegible]WG. [illegible]variectomy-induced bone loss varies among inbred strains of mice. *J Bone Miner Res*. 2005;20(7):1085–1092. doi:[illegible]1359/JBMR.0[illegible]07
23. Cook DA, Fellgett SW, Pownall ME, O'Shea PJ, Genever PG. Wnt-dependent [illegible]eogenic commitment of bone marrow stromal cells using a nov[illegible]GSK3β inhibitor. *Stem Cell Res*. 2014;12(2):415–427. doi:10.101[illegible]scr.2013.10.002
24. [illegible], Nguyen C, Ma H, et al. A small molecule inhibitor of beta-catenin/CREB-binding protein transcription [corrected]. *Proc [illegible] Acad Sci U S A*. 2004;101(34):12682–12687. doi:10.1073/pnas.0404875101
25. Rodan GA, Martin TJ. Therapeutic approaches to bone diseases. *Science*. 2000;289(5484):1508–1514. doi:10.1126/science.289.5484.1508
26. Ederveen AGH, Spanjers CPM, Quaijtaal JHM, Kloosterboer HJ. Effect of 16 months of treatment with tibolone on bone mass, turnover, and biomechanical quality in mature ovariectomized rats. *J Bone Miner Res*. 2001;16(9):1674–1681. doi:10.1359/jbmr.2001.16.9.1674
27. Jing H, Liao L, An Y, et al. Suppression of EZH2 prevents the shift of osteoporotic MSC fate to adipocyte and enhances bone formation during osteoporosis. *Mol Ther*. 2016;24(2):217–229. doi:10.1038/mt.2015.152
28. Moerman EJ, Teng K, Lipschitz DA, Lecka-Czernik B. Aging activates adipogenic and suppresses osteogenic programs in mesenchymal marrow stroma/stem cells: the role of PPAR-gamma2 transcription factor and TGF-beta/BMP signaling pathways. *Aging Cell*. 2004;3(6):379–389. doi:10.1111/j.1474-9728.2004.00127.x
29. Wu Q, Fu DX, Hou AJ, et al. Antioxidative phenols and phenolic glycosides from Curculigo orchioides. *Chem Pharm Bull (Tokyo)*. 2005;53(8):1065–1067. doi:10.1248/cpb.53.1065
30. Cichewicz RH, Nair MG. Isolation and characterization of stelladerol, a new antioxidant naphthalene glycoside, and other antioxidant glycosides from edible daylily (hemerocallis) flowers. *J Agric Food Chem*. 2002;50(1):87–91.
31. Almeida M, Han L, Martin-Millan M, O'Brien CA, Manolagas SC. Oxidative stress antagonizes Wnt signaling in osteoblast precursors by diverting beta-catenin from T cell factor- to forkhead box O-mediated transcription. *J Biol Chem*. 2007;282(37):27298–27305. doi:10.1074/jbc.M702811200

Supplementary materials

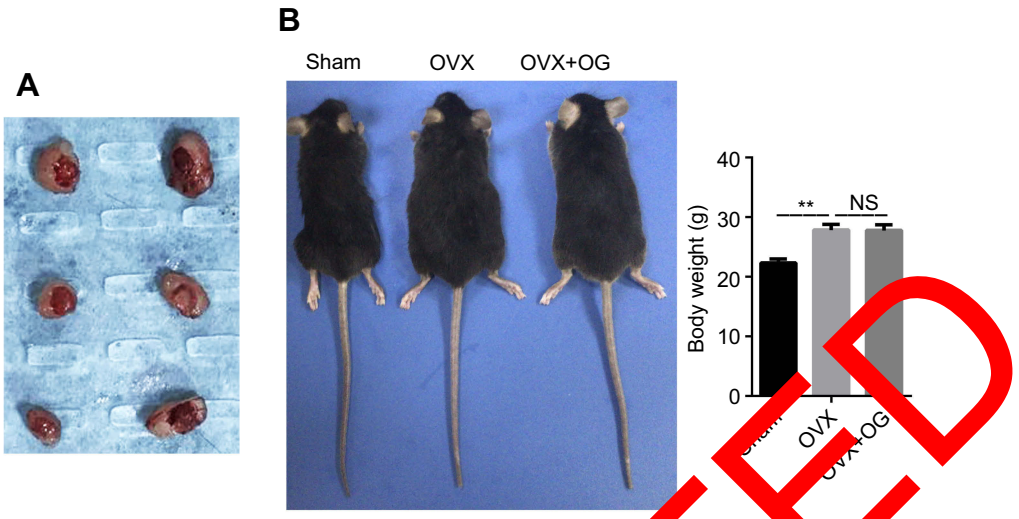

Figure S1 Establishment of OVX mouse model. (**A**) Photo of resected ovaries in mice. (**B**) Representative photo of fatty body of OVX mice 3 months after OVX and body weight measurement. **$p<0.01$. Plots show mean ± S.D.
Abbreviation: ns, not significant.

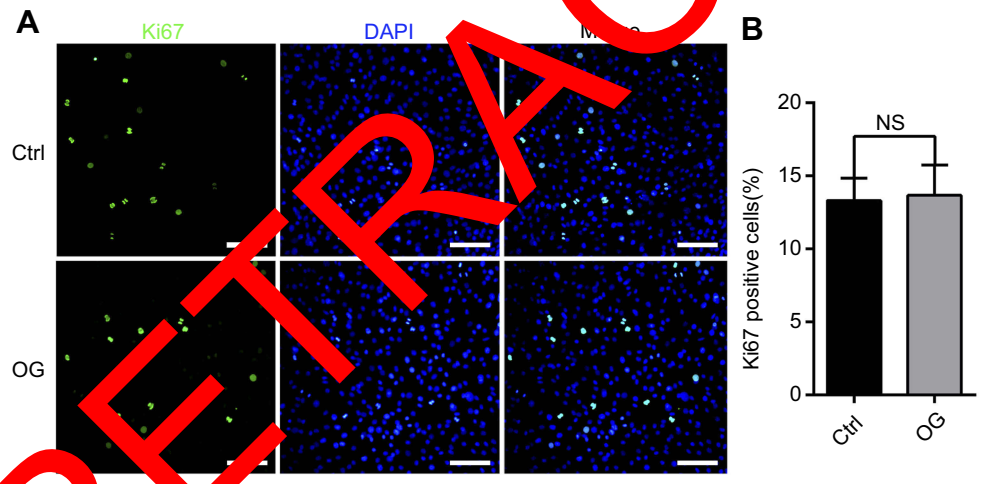

Figure S2 Immunostaining of Ki-67 in BMSCs treated with OG showed that OG did not affect BMSC proliferation.
Abbreviation: ns, not significant.

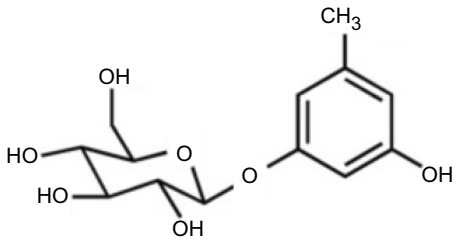

Figure S3 The chemical structure of OG.